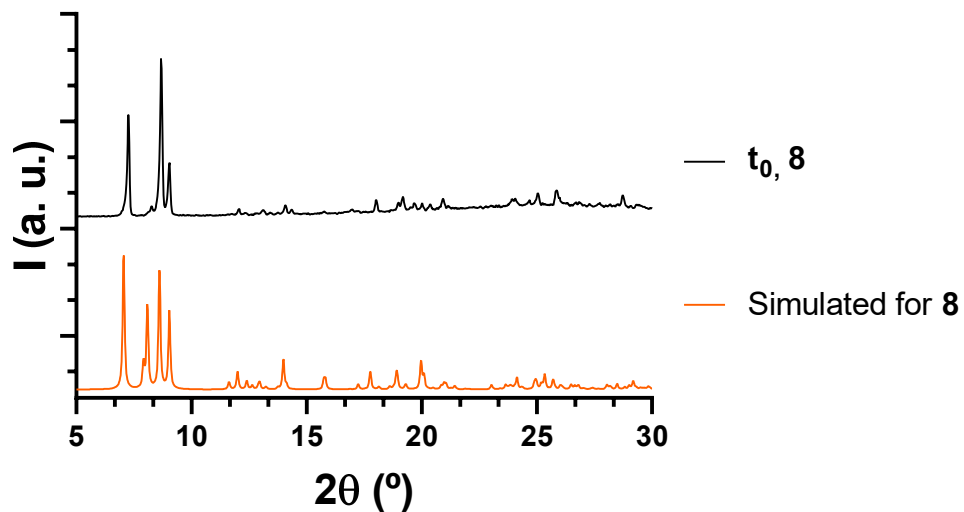


## SUPPORTING INFORMATION

**Magneto-thermal properties and slow magnetic relaxation in Mn(II)Ln(III)  
complexes: Influence of magnetic coupling on the magneto-caloric effect.**

Itziar Oyarzabal, Andoni Zabala-Lekuona, Antonio J. Mota, María A. Palacios, Antonio Rodríguez-Diéguéz, Giulia Lorusso, Marco Evangelisti, Corina Rodríguez-Esteban, Euan K. Brechin, José M. Seco and Enrique Colacio



**Fig. S1.-** For complex **8**, simulated pattern from single-crystal X-ray diffraction (orange line) and experimental PXRD recorded in mother liquor (black line).

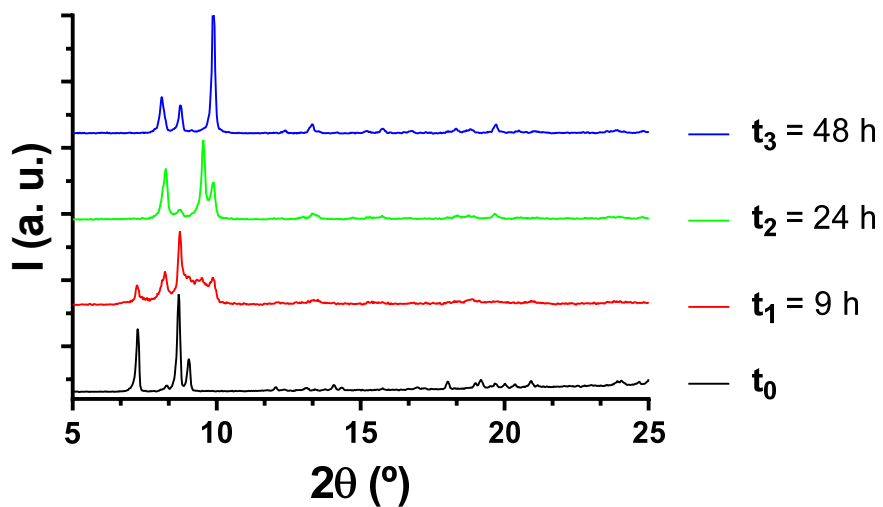


**Fig. S2.-** For complex **8**, experimental PXRD recorded in mother liquor (black line) and at different  $t$  values once removed from solution (red, green and blue lines).

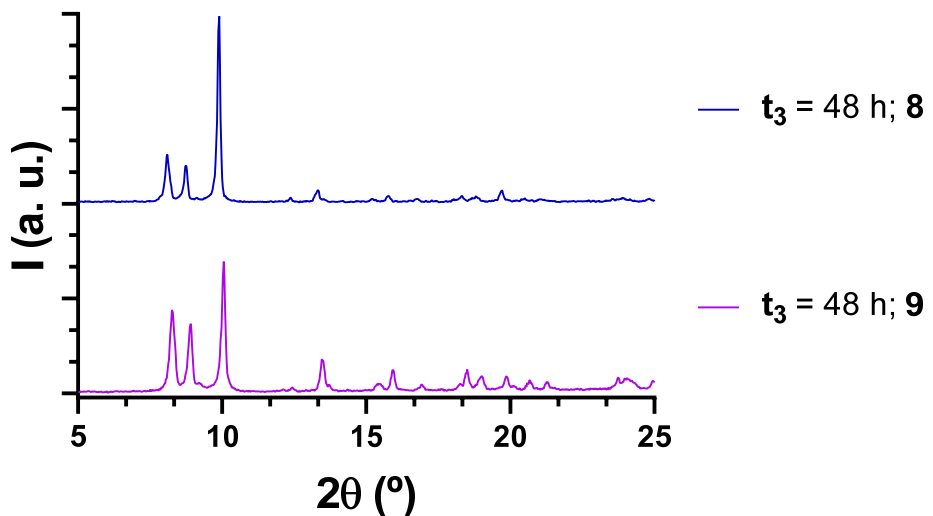


**Fig. S3.-** Experimental PXRD for compounds **8** (blue line) and **9** (purple line) once dried indicating a complete dehydration of the samples followed by a complete phase transformation.

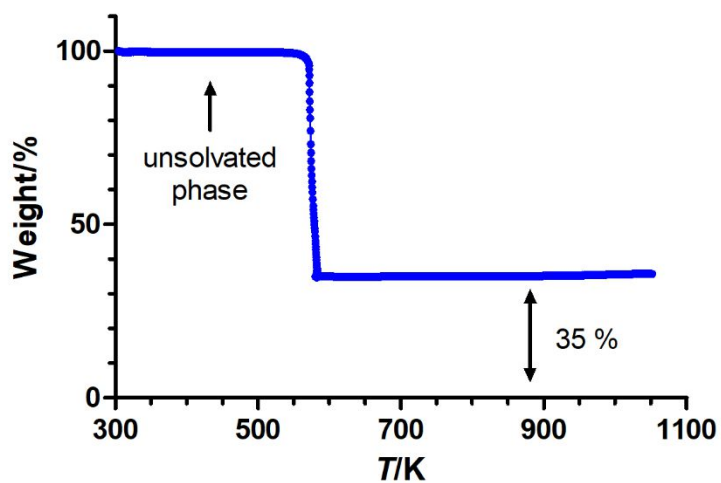


**Fig. S4.-** Thermogravimetric analysis (TGA) of complex **8** 48 h after filtering the crystals.

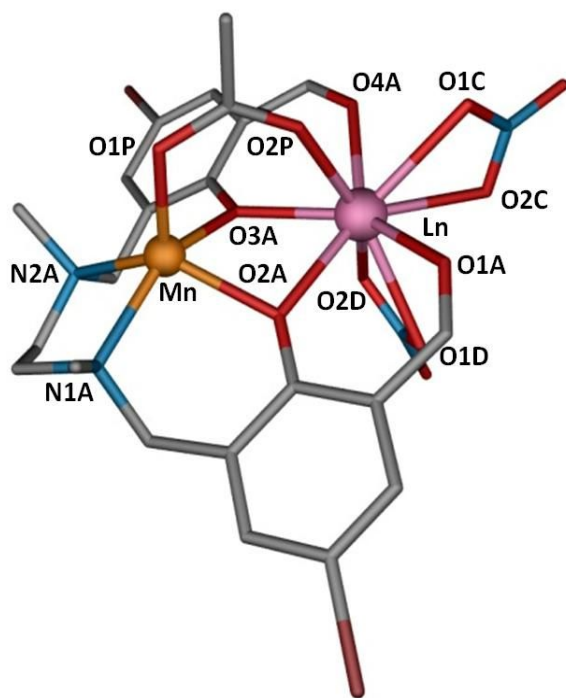


**Fig. S5.-** Perspective view of the molecular structure of complexes **1** and **2**. Hydrogen atoms are omitted for the sake of clarity. Colour code: N = blue, O = red, C = gray, Br = brown, Mn = orange, Ln = pink.

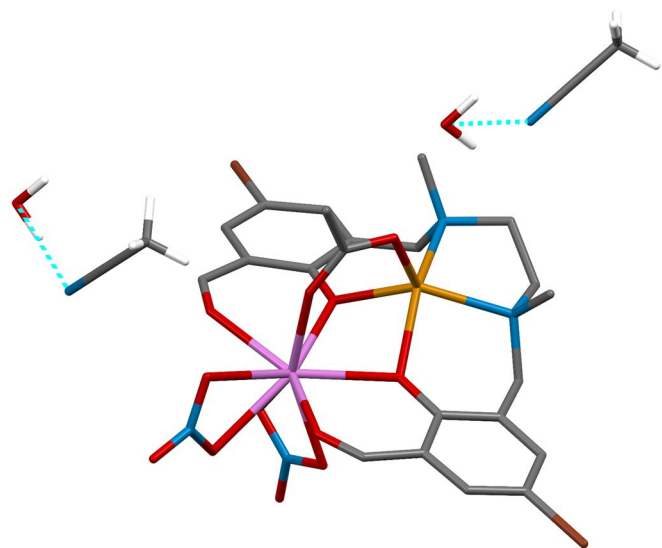


**Fig. S6.-** A perspective view of the structure of **1** together with intermolecular (blue dotted lines) hydrogen bonds.

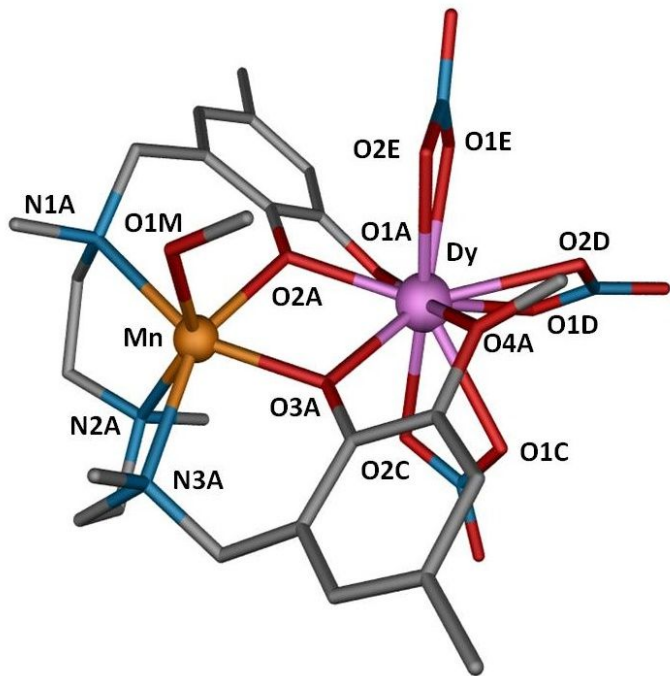


**Fig. S7.-** Perspective view of the molecular structure of complex **3**. Hydrogen atoms are omitted for the sake of clarity. Colour code: N = blue, O = red, C = gray, Mn = orange, Dy = pink.

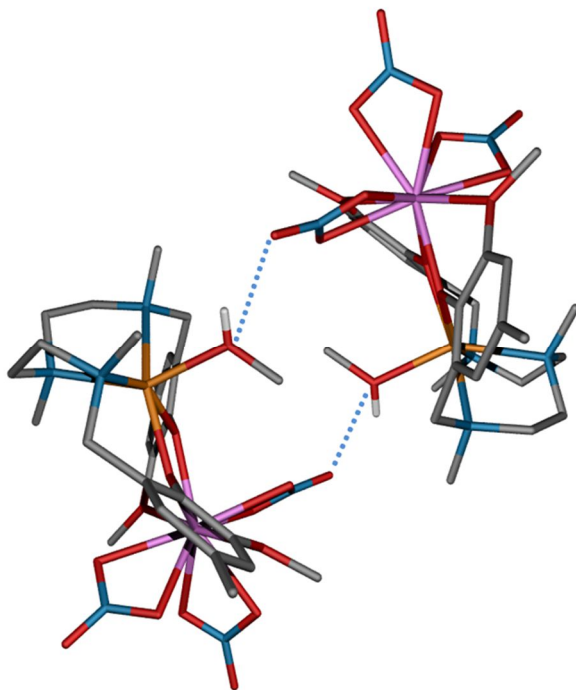


**Fig. S8.-** A perspective view of the structure of **3** together with intermolecular (blue dotted lines) hydrogen bonds.

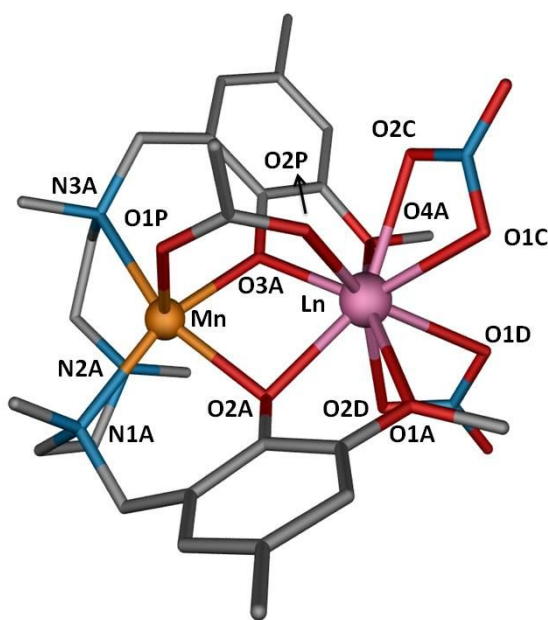


**Fig. S9.-** Perspective view of the molecular structure of complexes **4** and **5**. Hydrogen atoms are omitted for the sake of clarity. Colour code: N = blue, O = red, C = gray, Mn = orange, Ln = pink.

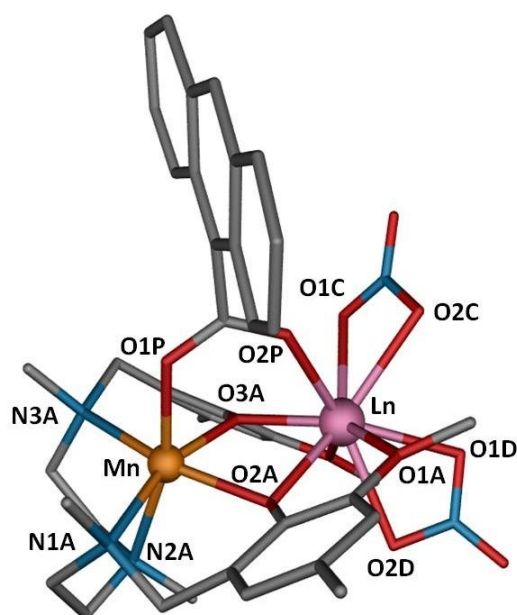


**Fig. S10.-** Perspective view of the molecular structure of complexes **6** and **7**. Hydrogen atoms and solvent molecules are omitted for the sake of clarity. Colour code: N = blue, O = red, C = gray, Mn = orange, Ln = pink.

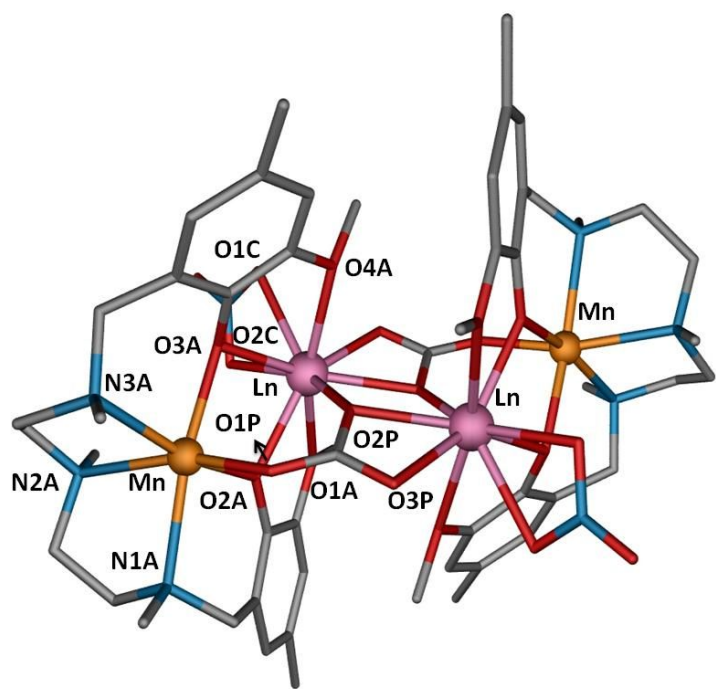


**Fig. S11.-** Perspective view of the molecular structure of complexes **8** and **9**. Hydrogen atoms and solvent molecules are omitted for the sake of clarity. Colour code: N = blue, O = red, C = gray, Mn = orange, Ln = pink.

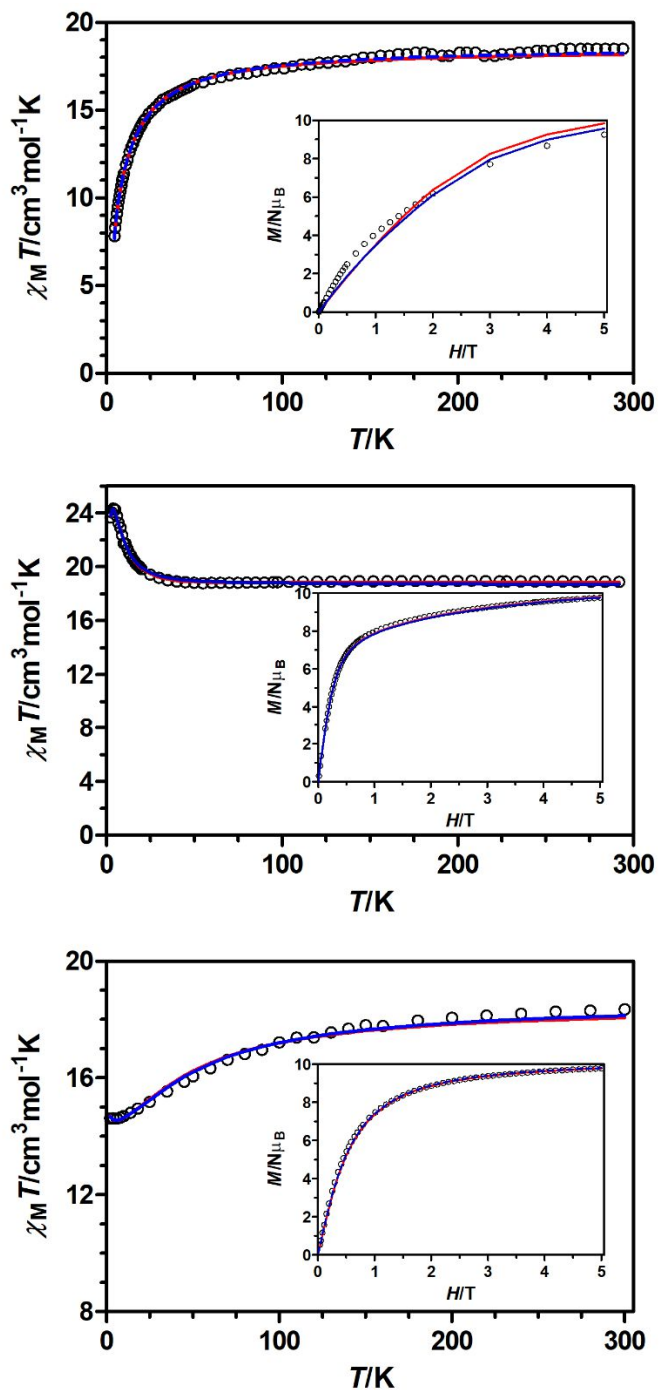


**Fig. S12.-** Temperature dependence of the  $\chi_M T$  product and field dependence of the magnetization at 2 K (inset) for **2** (top), **3** (middle) and **5** (bottom). Red and blue lines represent the best fits using the Hamiltonians in Equation 4 and 5, respectively.

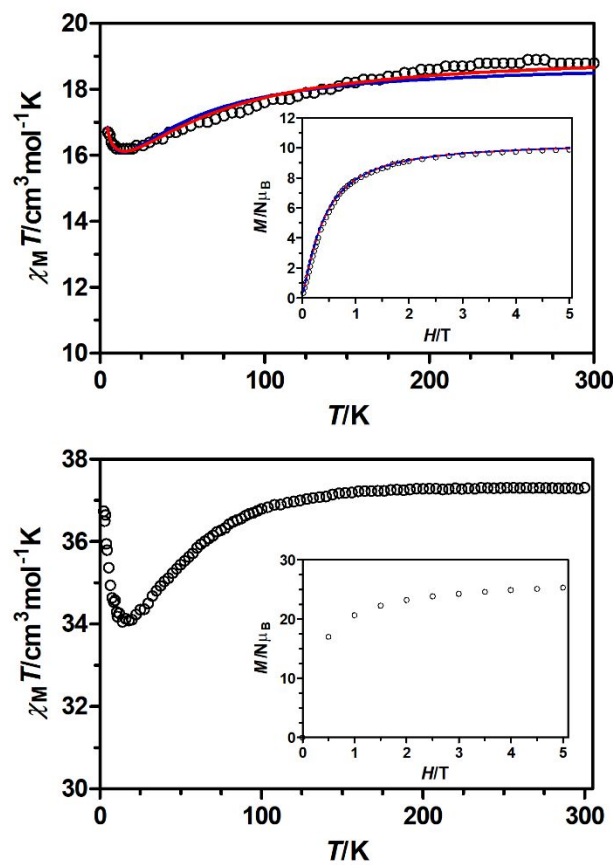


**Fig. S13.-** Temperature dependence of the  $\chi_M T$  product and field dependence of the magnetization at 2 K (inset) for **7** (top) and **9** (bottom). Red and blue lines represent the best fits using the Hamiltonians in Equation 4 and 5, respectively.

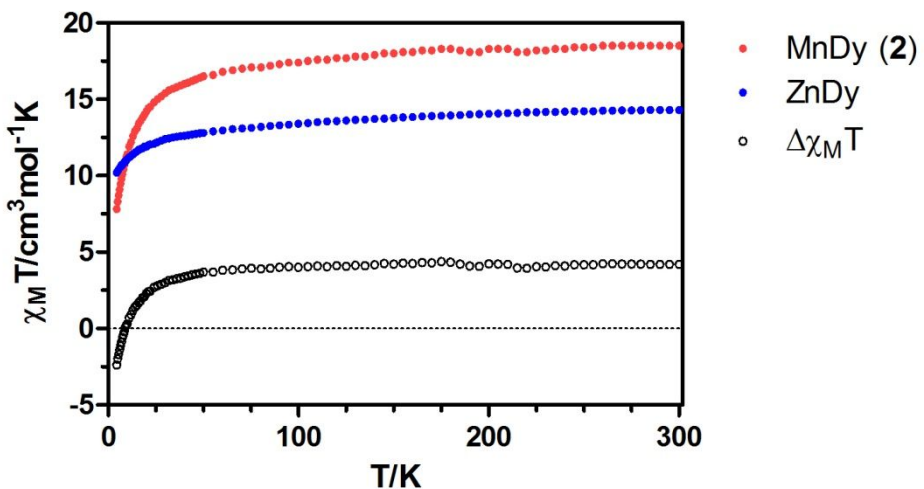


**Fig. S14.-** Temperature dependence of the  $\chi_M T$  product and the difference  $\Delta \chi_M T = \chi_M T_{(\text{MnDy})} - \chi_M T_{(\text{ZnDy})}$  for complex **2**.

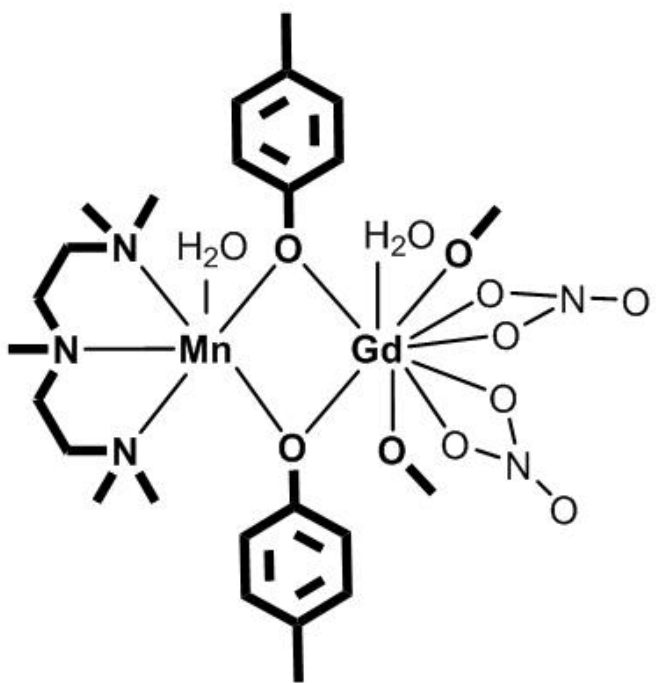


**Fig. S15.-** Schematic view of the model compound.

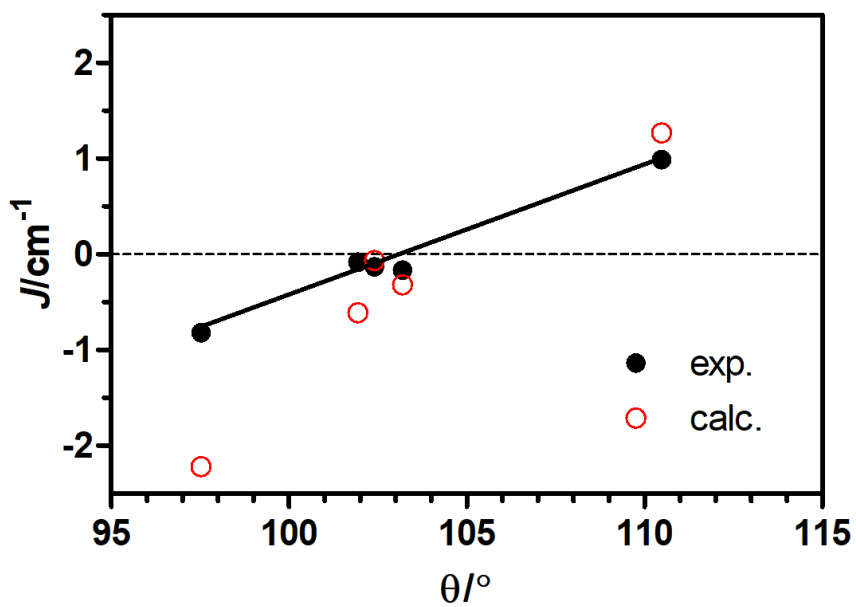


**Fig. S16.-** Scatter plot of experimental  $J$  (black circles) vs. the mean Mn-O-Gd angle ( $\theta$ ) for complexes prepared from ligands  $\text{H}_2\text{L}^1$  and  $\text{H}_2\text{L}^2$ . The open circles represent the values obtained from DFT calculations. The solid line represents the linear fitting of the experimental values.

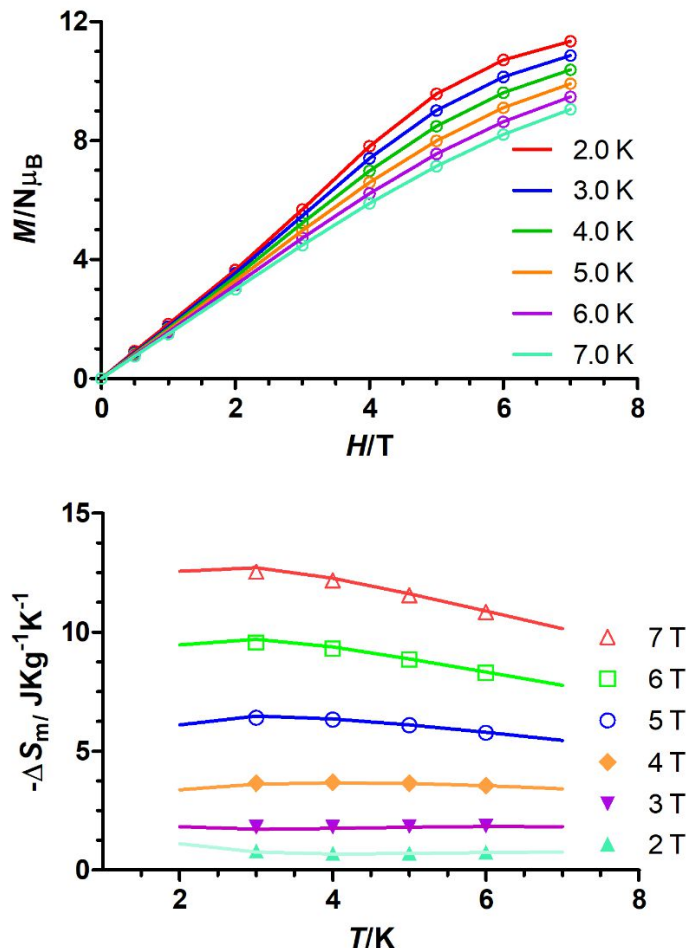


**Fig. S17.-** Isothermal field dependent curves for **1** between 2 and 7 K (top) and magnetic entropy changes (bottom) simulated with  $J = -0.82 \text{ cm}^{-1}$  and  $g = 2.00$  between 2 and 7 K (solid lines) and extracted from the experimental magnetization data with the Maxwell equation between 1 to 7 T and temperatures from 3 to 6 K (points).

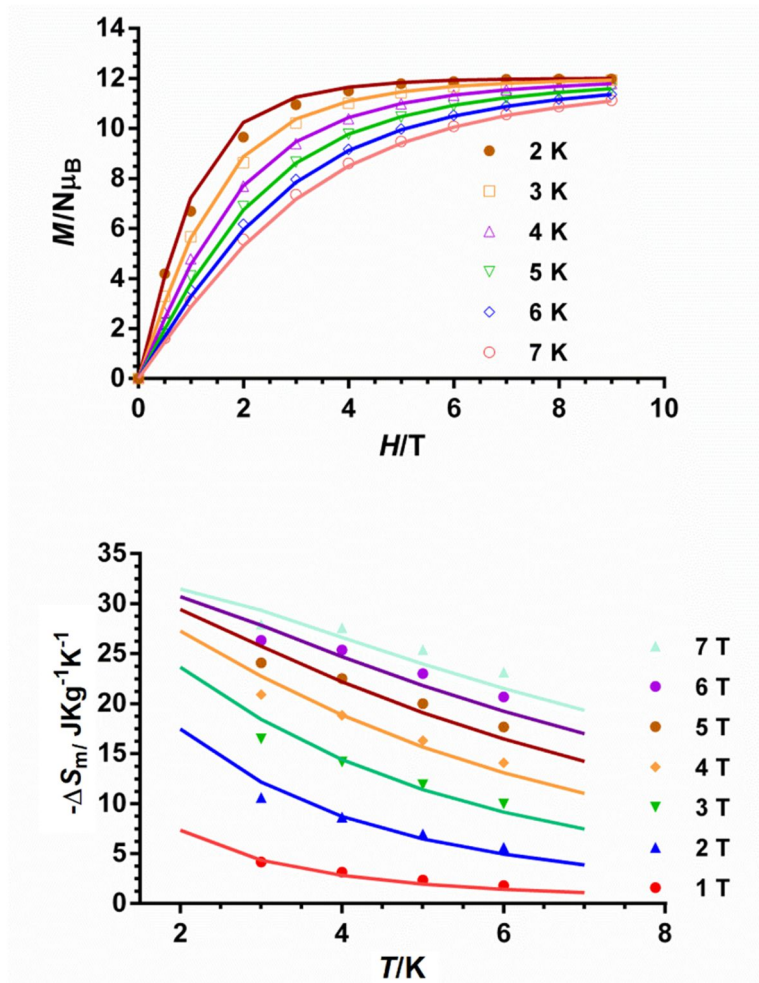


**Fig. S18.-** Isothermal field dependent curves for **4** between 2 and 7 K (top) and magnetic entropy changes (bottom) simulated with  $J = -0.08 \text{ cm}^{-1}$  and  $g = 2.00$  between 2 and 7 K (solid lines) and extracted from the experimental magnetization data with the Maxwell equation between 1 to 7 T and temperatures from 3 to 6 K (points).

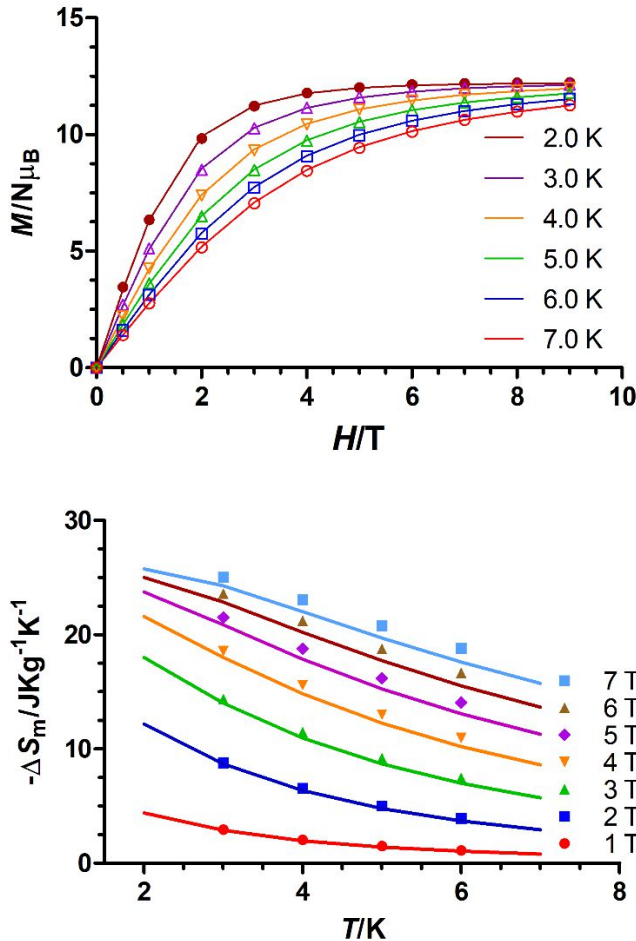


**Fig. S19.-** Isothermal field dependent curves for **6** between 2 and 7 K (top) and magnetic entropy changes (bottom) simulated with  $J = -0.16 \text{ cm}^{-1}$  and  $g = 2.03$  between 2 and 7 K (solid lines) and extracted from the experimental magnetization data with the Maxwell equation between 1 to 7 T and temperatures from 3 to 6 K (points).

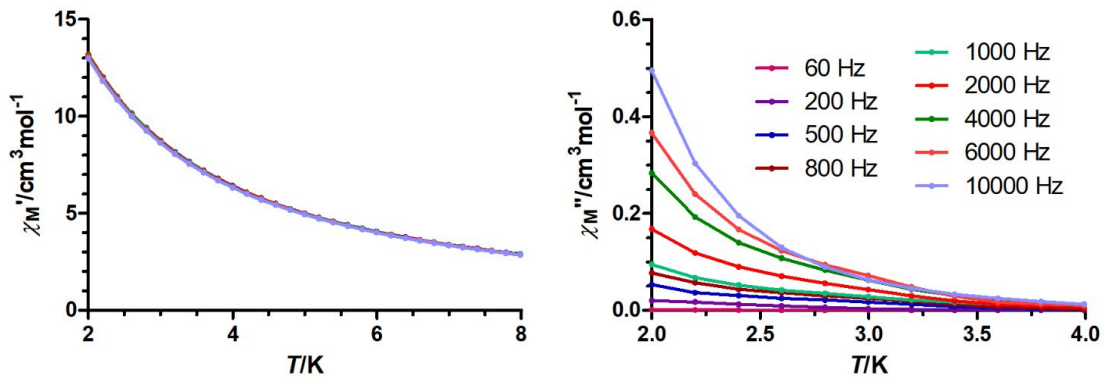


**Fig. S20.-** Temperature dependence of in-phase  $\chi_M'$  (left) and out-of phase  $\chi_M''$  (right) components of the *alternating current (ac)* susceptibility for complex **3** under zero *dc* applied field.

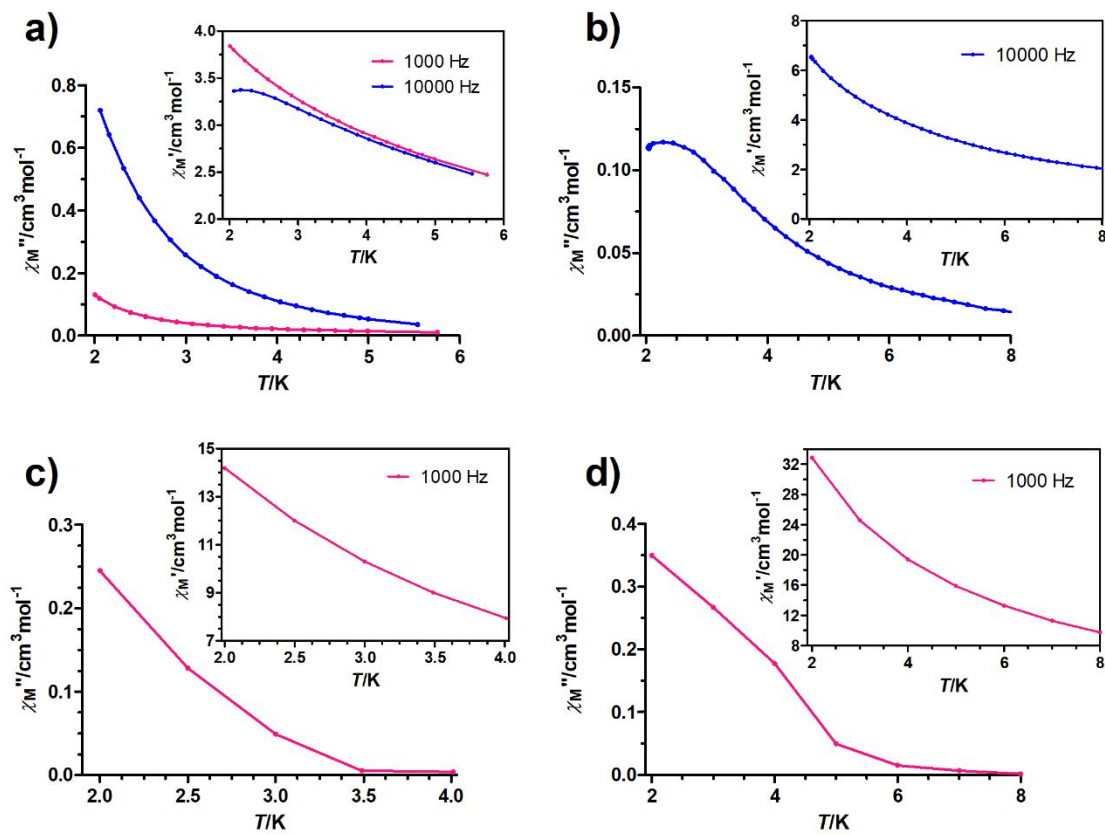


**Fig. S21.-** Temperature dependence of in-phase  $\chi_M'$  (inset) and out-of phase  $\chi_M''$  components of the *alternating current (ac)* susceptibility for complexes **2** (a), **5** (b), **7** (c) and **9** (d) under an applied field of 1000 Oe.

**Table S1.-** Crystallographic data.

Complex	1	2	3	4
Formula	C <sub>24</sub> H <sub>28</sub> Br <sub>2</sub> GdMnN <sub>5</sub> O <sub>13</sub>	C <sub>24</sub> H <sub>28</sub> Br <sub>2</sub> DyMnN <sub>5</sub> O <sub>13</sub>	C <sub>26</sub> H <sub>41</sub> DyMnN <sub>6</sub> O <sub>14</sub>	C <sub>27</sub> H <sub>40</sub> GdMnN <sub>5</sub> O <sub>12</sub>
M <sub>r</sub>	966.52	971.77	879.09	838.83
Crystal system	<i>Monoclinic</i>	<i>Monoclinic</i>	<i>Monoclinic</i>	<i>Monoclinic</i>
Space group (no.)	P2 <sub>1</sub> /n (14)	P2 <sub>1</sub> /n (14)	P2 <sub>1</sub> /n (14)	P2 <sub>1</sub> /n (14)
a (Å)	13.5996(4)	13.5722(2)	12.7783(8)	11.3864(7)
b (Å)	15.0087(4)	14.9625(2)	16.8706(11)	14.6689(7)
c (Å)	15.7090(5)	15.7042(2)	15.5190(10)	20.13390(10)
α (°)	90	90	90	90
β (°)	90.7330(10)	90.4760(10)	92.7364(12)	101.147(2)
γ (°)	90	90	90	90
V (Å <sup>3</sup> )	3206.14(16)	3189.01(8)	3341.7(4)	3299.4(3)
Z	4	4	4	4
D <sub>c</sub> (g cm <sup>-3</sup> )	2.002	2.024	1.747	1.689
μ(MoKa) (mm <sup>-1</sup> )	5.007	5.297	2.671	2.442
T (K)	100(2)	100(2)	100(2)	100(2)
Observed reflections	7727 (6641)	6600 (5979)	5872 (4936)	8425 (6097)
R <sub>int</sub>	0.0477	0.0362	0.0414	0.0515
Parameters	422	422	445	421
GOF	1.057	1.059	1.035	1.030
R <sub>I</sub> <sup>a,b</sup>	0.0328 (0.0246)	0.0287 (0.0244)	0.0443 (0.0343)	0.0859 (0.0531)
wR <sub>2</sub> <sup>c</sup>	0.0617 (0.0585)	0.0572 (0.0550)	0.0779 (0.0732)	0.1166 (0.1047)
Largest difference in peak and hole (e Å <sup>-3</sup> )	1.085 and -1.597	0.897 and -0.976	1.262 and -0.627	4.555 and -1.614

<sup>a</sup> R<sub>I</sub> = S||F<sub>o</sub>| - |F<sub>c</sub>||/S|F<sub>o</sub>|.<sup>b</sup> Values in parentheses for reflections with I > 2s(I).<sup>c</sup> wR<sub>2</sub> = {S[w(F<sub>o</sub><sup>2</sup> - F<sub>c</sub><sup>2</sup>)<sup>2</sup>] / S[w(F<sub>o</sub><sup>2</sup>)<sup>2</sup>]}<sup>1/2</sup>

**Table S1.-** Continuation.

Complex	5	6	7	8	9
Formula	C <sub>27</sub> H <sub>40</sub> DyMnN <sub>5</sub> O <sub>12</sub>	C <sub>44</sub> H <sub>52</sub> GdMnN <sub>7</sub> O <sub>12</sub>	C <sub>44</sub> H <sub>52</sub> DyMnN <sub>7</sub> O <sub>12</sub>	C <sub>56</sub> H <sub>94</sub> Gd <sub>2</sub> Mn <sub>2</sub> N <sub>8</sub> O <sub>26</sub>	C <sub>56</sub> H <sub>90</sub> Dy <sub>2</sub> Mn <sub>2</sub> N <sub>8</sub> O <sub>24</sub>
<i>M<sub>r</sub></i>	844.08	1083.11	1088.36	1719.77	1694.23
Crystal system	<i>Monoclinic</i>	<i>Monoclinic</i>	<i>Monoclinic</i>	<i>Triclinic</i>	<i>Triclinic</i>
Space group (no.)	<i>P2<sub>1</sub>/n</i> (14)	<i>P2<sub>1</sub>/n</i> (14)	<i>P2<sub>1</sub>/n</i> (14)	<i>P-1</i> (2)	<i>P-1</i> (2)
<i>a</i> (Å)	11.3886(6)	13.4699(19)	13.4614(16)	11.079(5)	10.702(2)
<i>b</i> (Å)	14.6602(7)	23.620(3)	23.617(3)	12.456(5)	12.462(3)
<i>c</i> (Å)	20.2613(11)	14.908(2)	14.8845(18)	14.319(5)	14.270(3)
<i>α</i> (°)	90	90	90	111.133(5)	111.316(3)
<i>β</i> (°)	101.593(2)	102.7733(16)	102.6754(12)	105.343(5)	104.241(3)
<i>γ</i> (°)	90	90	90	98.898(5)	98.203(3)
<i>V</i> (Å <sup>3</sup> )	3313.8(3)	4625.7(11)	4616.7(10)	1707.4(12)	1660.6(6)
<i>Z</i>	4	4	4	1	1
<i>D<sub>c</sub></i> (g cm <sup>-3</sup> )	1.692	1.555	1.566	1.673	1.694
<i>μ(MoKa)</i> (mm <sup>-1</sup> ) <sup>d</sup>	2.685	1.763	1.948	16.024	2.678
<i>T</i> (K)	100(2)	100(2)	100(2)	150.00(10)	100(2)
Observed reflections	8548 (6793)	8122 (7558)	8111 (7795)	6808 (5774)	5813 (4633)
<i>R<sub>int</sub></i>	0.0863	0.0246	0.0233	0.0634	0.0651
Parameters	421	595	595	433	426
GOF	1.025	1.037	1.051	1.015	0.998
<i>R<sub>1</sub></i> <sup>a,b</sup>	0.0484 (0.0289)	0.0262 (0.0240)	0.0212 (0.0203)	0.0641 (0.0534)	0.0645 (0.0457)
<i>wR<sub>2</sub></i> <sup>c</sup>	0.0592 (0.0551)	0.0600 (0.0585)	0.0511 (0.0505)	0.1411 (0.1320)	0.1052 (0.0975)
Largest difference in peak and hole (e Å <sup>-3</sup> )	1.397 and -0.980	0.940 and -0.474	0.993 and -0.341	1.809 and -1.415	1.873 and -0.884

<sup>a</sup>  $R_1 = \frac{\sum |F_o| - |F_c|}{\sum |F_o|}$ .<sup>b</sup> Values in parentheses for reflections with  $I > 2s(I)$ .<sup>c</sup>  $wR_2 = \left\{ \frac{\sum [w(F_o^2 - F_c^2)^2]}{\sum [w(F_o^2)^2]} \right\}^{1/2}$ <sup>d</sup>  $\mu(\text{CuKa})$  (mm<sup>-1</sup>) for **8**.

**Table S2.-** Selected bond lengths ( $\text{\AA}$ ) and angles ( $^\circ$ ).

Complex	1	2
Ln(1)-Mn(1)	3.414(1)	3.400(1)
Ln(1)-O(1A)	2.384(2)	2.354(2)
Ln(1)-O(2A)	2.394(2)	2.373(2)
Ln(1)-O(3A)	2.389(2)	2.364(2)
Ln(1)-O(4A)	2.392(2)	2.367(2)
Ln(1)-O(2P)bridge	2.329(2)	2.295(2)
Ln(1)-O(1C)nitrate	2.525(2)	2.517(2)
Ln(1)-O(2C)nitrate	2.470(2)	2.442(2)
Ln(1)-O(1D)nitrate	2.505(2)	2.480(2)
Ln(1)-O(2D)nitrate	2.478(2)	2.447(2)
Mn(1)-N(1A)	2.224(2)	2.230(2)
Mn(1)-N(2A)	2.227(2)	2.220(2)
Mn(1)-O(2A)	2.139(2)	2.140(2)
Mn(1)-O(3A)	2.148(2)	2.144(2)
Mn(1)-O(1P)bridge	2.060(2)	2.053(2)
Ln(1)-O(2A)-Mn(1)	97.59(7)	97.64(8)
Ln(1)-O(3A)-Mn(1)	97.48(7)	97.80(8)
O(2A)-Ln(1)-O(3A)	71.09(6)	71.30(7)
O(2A)-Ln(1)-O(2P)bridge	78.88(7)	79.58(8)
O(3A)-Ln(1)-O(2P)bridge	79.87(7)	80.54(8)
O(2A)-Mn(1)-O(3A)	80.89(7)	80.25(8)
O(2A)-Mn(1)-O(1P)bridge	104.54(7)	103.85(9)
O(3A)-Mn(1)-O(1P)bridge	101.58(8)	101.13(9)

**Table S2.-** Continuation.

<b>Complex</b>	<b>3</b>	<b>4</b>	<b>5</b>	<b>6</b>	<b>7</b>	<b>8</b>	<b>9</b>
Ln(1)-Mn(1)	3.661(1)	3.474(2)	3.462(1)	3.485(1)	3.466(1)	3.522(2)	3.498(1)
Ln(1)-Ln(1)						4.081(1)	4.063(1)
Ln(1)-O(1A)	2.556(3)	2.434(4)	2.421(2)	2.481(2)	2.461(2)	2.458(4)	2.437(4)
Ln(1)-O(2A)	2.312(3)	2.341(4)	2.329(2)	2.320(2)	2.290(2)	2.364(4)	2.331(4)
Ln(1)-O(3A)	2.291(3)	2.263(4)	2.236(2)	2.258(2)	2.231(2)	2.300(4)	2.266(4)
Ln(1)-O(4A)	2.611(3)	2.691(4)	2.723(2)	2.606(2)	2.601(2)	2.569(4)	2.567(4)
Ln(1)-O(1C)nitrate	2.464(3)	2.474(4)	2.445(2)	2.465(2)	2.433(2)	2.505(6)	2.485(5)
Ln(1)-O(2C)nitrate	2.468(3)	2.485(4)	2.460(2)	2.519(2)	2.497(2)	2.571(5)	2.528(4)
Ln(1)-O(1D)nitrate	2.487(3)	2.479(4)	2.456(2)	2.475(2)	2.440(2)		
Ln(1)-O(2D)nitrate	2.472(3)	2.497(4)	2.485(2)	2.507(2)	2.483(2)		
Ln(1)-O(1E)nitrate	2.517(3)						
Ln(1)-O(2E)nitrate	2.517(3)						
Ln(1)-O(2P)bridge		2.342(4)	2.317(2)	2.366(2)	2.344(2)	2.402(4)	2.382(4)
Ln(1)-O(2P)bridge						2.423(4)	2.420(4)
Ln(1)-O(3P)bridge						2.412(4)	2.375(4)
Mn(1)-N(1A)	2.377(3)	2.317(4)	2.323(2)	2.273(2)	2.271(2)	2.340(5)	2.333(5)
Mn(1)-N(2A)	2.295(4)	2.305(5)	2.307(2)	2.333(2)	2.332(2)	2.354(5)	2.341(5)
Mn(1)-N(3A)	2.365(3)	2.334(4)	2.332(2)	2.353(2)	2.348(2)	2.365(5)	2.362(5)
Mn(1)-O(2A)	2.146(3)	2.213(3)	2.205(2)	2.206(2)	2.205(2)	2.215(4)	2.199(4)
Mn(1)-O(3A)	2.152(3)	2.128(3)	2.139(2)	2.110(2)	2.115(2)	2.175(4)	2.184(4)
Mn(1)-O(1M)	2.217(3)						
Mn(1)-O(1P)bridge		2.108(4)	2.112(2)	2.156(2)	2.156(2)	2.126(4)	2.117(4)

**Table S2.-** Continuation.

<b>Complex</b>	<b>3</b>	<b>4</b>	<b>5</b>	<b>6</b>	<b>7</b>	<b>8</b>	<b>9</b>
Ln(1)-O(2A)-Mn(1)	110.36(11)	99.37(13)	99.53(7)	100.70(6)	100.89(5)	100.54(15)	101.06(15)
Ln(1)-O(3A)-Mn(1)	110.93(11)	104.51(15)	104.62(8)	105.80(6)	105.77(6)	103.80(17)	103.60(16)
Ln(1)-O(2P)-Ln(1)						115.52(15)	115.59(17)
O(2A)-Ln(1)-O(3A)	66.51(9)	72.45(12)	72.60(6)	71.77(5)	72.27(5)	73.95(14)	74.52(14)
O(2A)-Ln(1)-O(2P)bridge		78.91(13)	79.41(7)	77.99(5)	78.58(5)	75.18(14)	74.92(14)
O(2A)-Ln(1)-O(2P)bridge						137.32(14)	137.70(15)
O(3A)-Ln(1)-O(2P)bridge		80.14(13)	81.00(7)	79.45(6)	79.70(5)	74.41(15)	74.31(14)
O(3A)-Ln(1)-O(2P)bridge						106.34(14)	103.79(14)
O(2A)-Mn(1)-O(3A)	71.95(10)	77.62(13)	76.96(7)	76.86(6)	76.20(5)	79.43(15)	78.87(15)
O(2A)-Mn(1)-O(1P)bridge		91.68(14)	91.46(7)	91.84(6)	91.70(5)	93.71(16)	93.82(16)
O(3A)-Mn(1)-O(1P)bridge		95.61(15)	95.30(8)	93.42(6)	93.13(5)	89.36(16)	89.31(16)

**Table S3.**- Shape measures for  $\text{MnN}_2\text{O}_3$  coordination environments in complexes **1** and **2**.

Complex	PP-5	vOC-5	TBPY-5	SPY-5	JTBPY-5
<b>1</b>	31.455	3.183	3.590	0.731	6.531
<b>2</b>	31.297	3.272	3.616	0.806	6.521

\*PP-5: pentagon ( $D_{5h}$ ); vOC-5: vacant octahedron ( $C_{4v}$ ); TBPY-5: trigonal bipyramidal ( $D_{3h}$ ); SPY-5: square pyramid ( $C_{4v}$ ); JTBPY-5: Johnson trigonal bipyramidal ( $D_{3h}$ ).

**Table S4.**- Shape measures for  $\text{MnN}_3\text{O}_3$  coordination environments in complexes **3-9**.

Complex	HP-6	PPY-6	OC-6	TPR-6	JPPY-6
<b>3</b>	30.083	13.279	6.579	5.541	16.838
<b>4</b>	28.818	17.502	3.335	8.020	20.779
<b>5</b>	28.793	17.450	3.372	8.072	20.731
<b>6</b>	28.978	19.112	2.591	9.692	22.616
<b>7</b>	29.043	19.078	2.631	9.697	22.577
<b>8</b>	26.973	16.604	3.405	9.844	19.654
<b>9</b>	27.374	16.487	3.458	9.475	19.472

\*HP-6: hexagon ( $D_{6h}$ ); PPY-6: pentagonal pyramid ( $C_{5v}$ ); OC-6: octahedron ( $O_h$ ); TPR-6: trigonal prism ( $D_{3h}$ ); JPPY-6: Johnson pentagonal pyramid J2 ( $C_{5v}$ ).

**Table S5.-** Shape measures for  $\text{LnO}_9$  coordination environments in complexes **1**, **2** and **4-9**.

Complex	JCSAPR-9	CSAPR-9	JTCTPR-9	TCTPR-9	MFF-9
<b>1</b>	2.088	1.324	3.058	1.750	1.550
<b>2</b>	1.942	1.243	2.980	1.740	1.501
<b>4</b>	3.904	2.682	4.225	3.014	2.527
<b>5</b>	3.776	2.561	3.974	2.909	2.405
<b>6</b>	3.062	2.107	4.949	2.987	1.773
<b>7</b>	2.882	1.954	4.755	2.866	1.670
<b>8</b>	3.921	3.255	5.047	3.914	2.499
<b>9</b>	3.928	3.062	4.792	3.689	2.231

\*JCSAPR-9: capped square antiprism ( $C_{4v}$ ); CSAPR-9: spherical capped square antiprism ( $C_{4v}$ ); JTCTPR-9: tricapped trigonal prism ( $D_{3h}$ ); TCTPR-9: ( $D_{3h}$ ); spherical tricapped trigonal prism; MFF-9: muffin ( $C_s$ ).

\*Shape measures relative to other reference polyhedron are significantly larger.

**Table S6.-** Shape measures for  $\text{LnO}_{10}$  coordination environments in complex **3**.

Complex	JBCSAPR-10	JSPC-10	SDD-10	TD-10	HD-10
<b>3</b>	4.106	2.692	4.181	3.439	5.773

\*JBCSAPR-10: bicapped square antiprism J17 ( $D_{4d}$ ); JSPC-10: sphenocorona J87 ( $C_{2v}$ ); SDD-10: staggered dodecahedron ( $D_2$ ); TD-10: ( $C_{2v}$ ); tetradecahedron: HD-10: hexadecahedron ( $D_{4h}$ ).

\*Shape measures relative to other reference polyhedron are significantly larger.

**Table S7.-** Best fitting parameters of the magnetic data of complexes **2**, **3**, **5** and **7**.

Compounds	$ J\rangle$				$ LS\rangle$			
	<b>2</b>	<b>3<sup>b</sup></b>	<b>5</b>	<b>7</b>	<b>2</b>	<b>3<sup>b</sup></b>	<b>5</b>	<b>7</b>
$J_{\text{Mn(II)Dy(III)}} (\text{cm}^{-1})$	-0.84 (2)	1.46(3)	0.048(5)	0.16(1)	-0.90(1)	1.52(5)	0.046(3)	0.18(1)
$D_{\text{Ln}} (\text{cm}^{-1})$	5.25(3)	7.1(4)	14.1(3)	15.8(2)	39.0(9)	63(1)	120(1)	94(2)
$E_{\text{Ln}} (\text{cm}^{-1})$	0.4(1)	1.43(9)	1.32(7)	1.96(8)	1.45(1)	3.57(6)	3.4(1)	3.69(3)
$g_{\text{Ln}}^{\text{a}}$	1.33	1.33	1.33	1.35				
$g_{\text{Mn}}^{\text{a}}$	2.0	2.05	2.0	2.05	2.0	2.05	2.0	2.05
$\sigma_{\text{Ln}}$					0.999(1)	0.999(1)	0.998(1)	1.000(1)

<sup>a</sup>These values were fixed to the indicated values. <sup>b</sup> A mean field intermolecular interaction of  $zJ = -0.002 \text{ cm}^{-1}$  was considered.

**Table S8.-** Maximum magnetic entropy change for Mn and Gd-based complexes found in the literature.

Complex	$-\Delta S_m (\text{JKg}^{-1}\text{K}^{-1}) (7 \text{ T})$	Dimensionality	T (K)	Ref.
Complex <b>8</b>	36.4	0D	2.2	T.w.
$\text{Gd}_2\text{Mn}_2(\mu_3\text{-OH})_2\text{L}^6(\text{NO}_3)_4 \cdot \text{CH}_3\text{CN}$	40.59	0D	2	31
$[\text{GdMn}_{0.5}(\text{OAc})_4(\text{H}_2\text{O})_2] \cdot 3\text{H}_2\text{O}$	38.7	1D	2.5	31
$\{[\text{Gd}_5\text{Mn}(\text{L}^7)_3(\text{H}_2\text{O})_{10}(\mu_3\text{-OH})_6](\text{NO}_3)_5 \cdot 13\text{H}_2\text{O}\}_n$	38.3	3D	2	31
$[\text{Mn}(\text{H}_2\text{O})_6][\text{MnGd}(\text{oda})_3]_2 \cdot 6\text{H}_2\text{O}$	50.1	3D	1.8	31
$\{(\text{H}_3\text{O})_3[\text{Gd}_3\text{Mn}_2(\text{Trz})_4] \cdot 12\text{H}_2\text{O}\}_n$	40.3	3D	2	31
$\{[\text{Gd}_4\text{Mn}(\text{L}^7)_3(\text{H}_2\text{O})_3(\mu_3\text{-OH})_4(\text{HCOO})_{1.5}] \cdot (\text{NO}_3)_{2.5} \cdot 6\text{H}_2\text{O}\}_n$	46.0	3D	2	31

T.w. = this work.

$\text{HL}^6$  = methyl 3-methoxysalicylate

OAc = acetate

$\text{H}_2\text{L}^7$  = 2,2'-dipyridine-4,4'-dicarboxylic acid

Oda = oxydiacetate

Trz =  $\text{H}_4\text{Trz}$  = tri(1H-tetrazole-5-yl)methanol